

**DTIC FILE COPY**

(2)

**RADC-TR-89-274**  
**In-House Report**  
**November 1989**

**AD-A226 219**



# **ANALYTIC RAY TRACING USING ERMAKOV INVARIANTS**

**Stanford P. Yukon**

**DTIC**  
**ELECTE**  
**SEP 07 1990**  
**S D**

**APPROVED FOR PUBLIC RELEASE; DISTRIBUTION UNLIMITED.**

**ROME AIR DEVELOPMENT CENTER**  
**Air Force Systems Command**  
**Griffiss Air Force Base, NY 13441-5700**

This report has been reviewed by the RADC Public Affairs Office (PA) and is releasable to the National Technical Information Service (NTIS). At NTIS it will be releasable to the general public, including foreign nations.

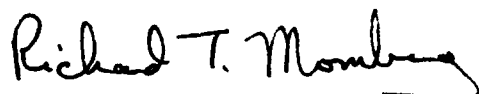
RADC TR-89-274 has been reviewed and is approved for publication.

APPROVED:



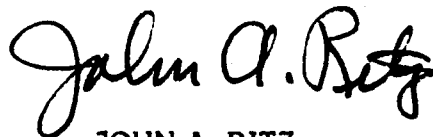
J. LEON POIRIER  
Chief, Applied Electromagnetics Division  
Directorate of Electromagnetics

APPROVED:



RICHARD T. MOMBERG, Lt Col, USAF  
Deputy Director  
Directorate of Electromagnetics

FOR THE COMMANDER:



JOHN A. RITZ  
Directorate of Plans and Programs

If your address has changed or if you wish to be removed from the RADC mailing list, or if the addressee is no longer employed by your organization, please notify RADC (EECP) Hanscom AFB MA 01731-5000. This will assist us in maintaining a current mailing list.

Do not return copies of this report unless contractual obligations or notices on a specific document requires that it be returned.

REPORT DOCUMENTATION PAGE			Form Approved OMB No. 0704-0188	
Public reporting for this collection of information is estimated to average 1 hour per response, including the time for reviewing instructions, searching existing data sources, gathering and maintaining the data needed, and completing and reviewing the collection of information. Send comments regarding this burden estimate or any other aspect of this collection of information, including suggestions for reducing this burden, to Washington Headquarters Services, Directorate for Information Operations and Reports, 1215 Jefferson Davis Highway, Suite 1204, Arlington, VA 22202-4302, and to the Office of Management and Budget, Paperwork Reduction Project (0704-0188), Washington, DC 20503.				
1. AGENCY USE ONLY (Leave blank)		2. REPORT DATE Nov 89		3. REPORT TYPE AND DATES COVERED In-House Dec 86 - Dec 88
4. TITLE AND SUBTITLE Analytic Ray Tracing Using Ermakov Invariants			5. FUNDING NUMBERS PE 62702F, 61102F PR 4600, 2305 TA 16, J2 WU 08, 01	
6. AUTHOR(S) Yukon, Stanford P.			8. PERFORMING ORGANIZATION REPORT NUMBER RADC TR-89-274	
7. PERFORMING ORGANIZATION NAME(S) AND ADDRESS(ES) Rome Air Development Center/EECP Hanscom AFB Massachusetts 01731-5000				
9. SPONSORING/MONITORING AGENCY NAME(S) AND ADDRESS(ES)			10. SPONSORING/MONITORING AGENCY REPORT NUMBER	
11. SUPPLEMENTARY NOTES				
12a. DISTRIBUTION/AVAILABILITY STATEMENT Approved for public release, distribution unlimited.			12b. DISTRIBUTION CODE	
13. ABSTRACT (Maximum 200 words) A method for the rapid generation of raypaths and ionograms in model ionospheres is presented. The ionosphere is first cast into the form of a soluble potential well with range dependent parameters. An analytic calculation of raypaths may then be carried out in the paraxial approximation using the theory of Ermakov invariants. The correspondence of rays to full wave coherent states and the possibility of ionospheric convergence zones is discussed. <i>100 words</i>				
14. SUBJECT TERMS Raytracing      Ducted Propagation      Paraxial approximation Ionosphere      High frequency      Parabolic approximation Potential well      IONCAP      Scalar wave equation			15. NUMBER OF PAGES 40	
17. SECURITY CLASSIFICATION OF REPORT UNCLASSIFIED			16. PRICE CODE	
18. SECURITY CLASSIFICATION OF THIS PAGE UNCLASSIFIED		19. SECURITY CLASSIFICATION OF ABSTRACT UNCLASSIFIED		20. LIMITATION OF ABSTRACT

## Preface

I wish to thank Dr. Chu-Hsien Lin for his help in uncovering and overcoming some of the numerical pitfalls in the use of IONCAP and the Jones-Stephenson code and for similar aid to the current program. I would like to thank Jewel Holst for her patient help in programming the current model and searching out its bugs.



Accession For	
NTIS CRA&I	<input checked="" type="checkbox"/>
DTIC TAB	<input type="checkbox"/>
Unannounced	<input type="checkbox"/>
Justification	
By	
Distribution /	
Availability Codes	
Dist	Avail and/or Special
A-1	

## Contents

1. INTRODUCTION	1
2. RAY TRACING AND THE TIME-DEPENDENT SCHROEDINGER EQUATION	3
3. A MORSE POTENTIAL MODEL FOR THE E-F LAYER TROUGH	8
4. COHERENT STATES AND RAY PATHS FOR THE MORSE POTENTIAL	15
4.1 Coherent States of the Morse Potential	17
4.2 Focusing Properties of the Morse Potential	19
5. RAY TRACING IN THE IONCAP IONOSPHERE	22
REFERENCES	33

## Illustrations

1. Plot of the Effective Ionospheric Potential $V_{CH}(x)$ as a Function of Height $x$ .	9
2. Plot of the Morse Potential $V_M(x) = \gamma^2 (e^{\alpha x} - 1)^2$ as a Function of Height $x$ with $\gamma^2 = 1$ and $\alpha = 1$ .	12
3. Plot of the Munk Profile and Ray Convergence Zones from Reference 16.	20
4. Plot of the IONCAP Effective Ionospheric Potential $V_E(x)$ as a Function of Height $x$ .	23
5. The IONCAP Potential of Figure 4 broken up into Sector Potential Wells I through IV.	25
6. Three Possible Cases for Turning Point Behavior Near a Sector Boundary.	26
7. Ray Traces Using Current Model vs Jones-Stephenson's <sup>1</sup> Program for Frequency = 16 MHz, Takeoff Angle = 7.1°.	28
8. Ray Traces Using Current Model vs Jones-Stephenson's <sup>1</sup> Program for Frequency = 16 MHz, Takeoff Angle = 6.7°.	29
9. Ray Traces Using Current Model vs Jones-Stephenson's <sup>1</sup> Program for Frequency = 16 MHz, Takeoff Angle = 6.4°.	30
10. Ionogram Produced Using Current Ray Tracing Model with Transmitter Location and Time as Shown in Figure 7.	31
11. Ionogram Produced Using Jones-Stephenson's <sup>1</sup> Program with Transmitter Location and Time as Shown in Figure 7.	32

# Analytic Ray Tracing Using Ermakov Invariants

## 1. INTRODUCTION

The impetus for developing a computational technique capable of rapidly producing ray traces and ionograms came from the requirements of an experiment designed to measure HF propagation in the ionospheric E-F<sub>2</sub> duct in situ. In the experiment, a receiver placed on a polar orbiting satellite is to detect 6-30 MHz signals injected into the duct either by means of naturally occurring ionospheric gradients or by scattering from an artificially heated ionospheric volume. Since a time delay vs frequency ionogram will change depending on position in the orbit, a capability for producing essentially real-time ionograms is needed to direct the experiment efficiently.

Programs exist that can numerically integrate the differential equations of motion (such as the Haselgrove Hamiltonian equations) that describe a propagating ray.<sup>1</sup> Depending on the path length, the time required to produce an ionogram on a mainframe computer can run from 20-200 minutes. The time required to evaluate an ionogram using the analysis to follow will require less than 100 seconds and can be run on small computers.

---

(Received for Publication 14 Nov. 1989)

<sup>1</sup> Jones, R.M., Stephenson, J.J. (1975) A Versatile Three-Dimensional Ray Tracing Computer Program for Radio Waves in the Ionosphere, *U.S. OT Report*, 75-76.

The method developed here starts from a description of propagating HF waves by the scalar wave equation in the paraxial approximation, which is valid if changes in the ionosphere are small over distances on the order of a wavelength ( $\lambda \approx 10\text{-}50\text{m}$ ). By redefining  $z$ , the distance along the great circle path as a time coordinate, the paraxial equation can be cast in the form of the time dependent Schroedinger equation.

The time dependent Schroedinger equation has recently been shown to be soluble for a certain class of potentials by Ermakov invariant theory.<sup>2</sup> This class consists of potentials obtained by canonical transformations that are parametrized by functions that obey a set of time-dependent differential constraints. By approximating a path-dependent ionospheric potential, such that it satisfies these constraints, exact time-dependent scalar wave solutions to the approximating ionospheric potential may be obtained.

Since it is difficult to find soluble double-well potentials that can approximate the ionosphere over extended ranges, as a practical matter it is necessary to join two (or more) single-well potentials at a common boundary to model the total ionospheric potential. A consistent calculation can then be made in the ray approximation, which corresponds to solving Newton's equations of motion for a particle in a time-dependent one-dimensional potential well. By approximating the ionospheric potential along a great circle path by joined single-well potentials, such that each satisfies the differential constraints of Ermakov theory, the solution to the ray tracing problem is mapped onto the problem of solving for the equations of motion of a particle in a static potential.

By choosing the fitting potential to be a combination of Morse and linear potentials or quadratic and linear potentials or any potential with known solutions that when shifted and scaled conforms to the ionospheric potential over the chosen range, a good approximation for the entire ray tracing problem may thus be obtained analytically. The approximations that inhere in this method of tracing rays in a model ionosphere enter through the choice of the fitting potential, the paraxial approximation, and the fact that the differential constraint equations are only approximately obeyed.

The outline of this report is as follows: In Section 2 we indicate how the paraxial approximation to the scalar wave equation may be viewed as a time-dependent Schroedinger equation. The use of Ermakov invariant theory for solving the time-dependent Schroedinger equation is then outlined. In Section 3 we discuss how the application of the time-dependent Schroedinger formalism may be applied to the ionospheric ray tracing problem by using Morse and linear potentials to fit the ionosphere. The possibility of using double-well potentials obtained through the Darboux transformation is also discussed. In Section 4 we discuss the relation of coherent states of the time-dependent Schroedinger equation and rays for the Morse potential. The possibility of multiple focusing of rays is pointed out. This behavior is analogous to convergence zones in the case of ocean acoustic ducts and provides an explanation for both cases. In Section 5 we discuss ray tracing in the potential wells provided

---

<sup>2</sup> Ray, J.R. (1982) Exact Solutions to the Time-Dependent Schroedinger Equation, *Phys. Rev.*, **A26**:729/Hartley, J.G., Ray, J.R. (1981) Ermakov Systems and Quantum-Mechanical Superposition Laws, *Phys. Rev.*, **A24**:2873.



directly by IONCAP.<sup>3</sup> Examples of ray traces and ionograms calculated both by the Jones-Stephenson ray tracing program using IONCAP and by the present method are given.

## 2. RAY TRACING AND THE TIME-DEPENDENT SCHROEDINGER EQUATION

Our description of ionospheric HF propagation starts from the scalar wave equation for a transverse electric field component. For propagation along a great circle path this can be written as

$$\frac{\partial^2 E}{\partial r^2} + \frac{1}{r} \frac{\partial E}{\partial r} + \frac{1}{r^2} \frac{\partial^2 E}{\partial \phi^2} + k_0^2 n^2(r, \phi) E(r, \phi) = 0 \quad (1)$$

$$\text{with } k_0 = \frac{\omega}{c}.$$

Assuming a solution of the form

$$E(r, \phi) = E(r, \phi) e^{i\tilde{\beta}\phi}. \quad (2)$$

This can be written as

$$\frac{\partial^2 E}{\partial r^2} + \frac{1}{r} \frac{\partial E}{\partial r} + \frac{1}{r^2} \frac{\partial^2 E}{\partial \phi^2} + 2i\tilde{\beta} \frac{\partial E}{\partial \phi} - \frac{\tilde{\beta}^2 E}{r^2} + k_0^2 n^2(r, \phi) E(r, \phi) = 0. \quad (3)$$

In terms of the coordinates for height  $x$  above the Earth's surface  $x = r - R_0$  where  $R_0$  is the Earth's radius, and range  $z$  along the great circle path at the Earth's surface  $z = R_0\phi$ , this can be rewritten as

<sup>3</sup> Lloyd, J.L., Haydon, G.W., Lucas, D.L., and Teters, L.R. (1984) Estimating the Performance of Telecommunications Systems Using the Ionospheric Transmission Channel, Vol. 1, *Techniques for Analyzing Ionospheric Effects Upon HF Systems*, NTIA/ITS.

$$\frac{\partial^2 E}{\partial x^2} + \frac{1}{(R_0 + x)} \frac{\partial E}{\partial x} + \frac{1}{(1 + x/R_0)^2} \frac{\partial^2 E}{\partial z^2} + \frac{2i\beta k_0}{(1 + x/R_0)^2} \frac{\partial E}{\partial z} - \frac{\beta^2 k_0^2 E}{(1 + x/R_0)^2} + k_0^2 n^2 E = 0 \quad (4)$$

where the angular momentum  $\tilde{\beta}$  has been re-expressed as

$$\tilde{\beta} = \beta k_0 R_0. \quad (5)$$

Since derivatives in height occur on a scale of tens of km, the term  $\frac{1}{(R_0 + x)} \frac{\partial E}{\partial x}$  may be neglected in comparison with the term  $\frac{\partial^2 E}{\partial x^2}$ . If we assume that changes in  $n(x, z)$  (and  $E(x, z)$ ) occur on a scale much larger than the wavelength  $\lambda (= 2\pi/k_0)$  of the propagating wave, then we may neglect terms operated on by  $\partial/\partial z$  in comparison to those multiplied by  $i\beta k_0$ . Expanding the remaining terms to lowest order in  $x/R_0$  yields the approximate wave equation

$$\frac{i}{k_0} \beta \frac{\partial \epsilon}{\partial z} = -\frac{1}{2k_0^2} \frac{\partial^2 \epsilon}{\partial x^2} - \left[ \frac{n^2(x, z)}{2} - \frac{\beta^2 x}{R_0} - \frac{\beta^2}{2} \right] \epsilon(x, z) \quad (6)$$

which is in the form of the time-dependent Schroedinger equation with  $k_0^{-1}$  replacing  $\hbar$ ,  $z/\beta$  replacing the time variable  $\tau$ , and with the time-dependent potential  $V_1(x, \tau)$  given by

$$V_1(x, \tau) = - \left[ \frac{n^2(x, \tau)}{2} - \frac{\beta^2 x}{R_0} - \frac{\beta^2}{2} \right]. \quad (7)$$

For the ionosphere, the dielectric constant is given by

$$n^2(x, z) = \epsilon(x, z) = 1 - \frac{v_p^2(x, z)}{v^2} \quad (8)$$

where  $\nu_p(x,z)$  is the local plasma frequency and  $\nu$  is the wave frequency. Methods have been developed within the past few years for dealing with time-dependent Hamiltonians by using the method of Ermakov invariants<sup>2</sup> or equivalently by a rescaling of space and time variables in conjunction with a unitary transformation of the wave function.<sup>2,4</sup> The most general potential that can be dealt with by these methods must be expressible in the form

$$V_E(x,\tau) = \nu [(x - \sigma(\tau)) / \rho(\tau)] / \rho^2(\tau) + g_0(\tau) + x \cdot g_1(\tau) + x^2 \cdot g_2(\tau). \quad (9)$$

Where the scaling function  $\rho(\tau)$  and shift function  $\sigma(\tau)$  must obey the differential constraint conditions

$$\ddot{\rho}(\tau) + 2g_2(\tau)\rho(\tau) = \kappa/\rho^3(\tau) \quad (10)$$

$$\ddot{\sigma}(\tau) + 2g_2(\tau)\sigma(\tau) + g_1(\tau) = 0 \quad (11)$$

with  $\kappa$  an arbitrary constant and with  $g_0$ ,  $g_1$ , and  $g_2$  arbitrary functions of time.

The equations of motion for a ray (or a classical particle) equivalent to the wave Eq. (6) with a potential given by Eq. (9) are

$$\frac{d^2x}{dt^2} = -2g_2(\tau)x - g_1(\tau) - \frac{d\nu(x,\tau)}{dx} \frac{1}{\rho^3(\tau)}. \quad (12)$$

The Ermakov invariant for this system is given by

$$I = \frac{1}{2} [(\dot{x} - \dot{\sigma})\rho - \dot{\rho}(x - \sigma)]^2 + \nu((x - \sigma)/\rho). \quad (13)$$

---

<sup>4</sup> Lewis, H.R., and Leach, P.G.L. (1982) Exact Invariants for Time-Dependent Nonlinear Hamiltonian Systems, *Nonlinear Problems: Present and Future*, Bishop, A.R., Campbell, D.K., and Nicolaenko, B. (eds) p. 133, North Holland.

If  $x$  and  $t$  are transformed as

$$x' = \frac{x - \sigma(\tau)}{\rho(\tau)} \quad (14)$$

and

$$\tau' = \int_0^\tau \frac{d\tau''}{\rho^2(\tau'')} \quad (15)$$

the equations of motion and Ermakov invariant are transformed to

$$\frac{d^2 x'}{d\tau'^2} = -\kappa x' - \frac{dv(x')}{dx'} \quad (16)$$

and

$$I' = \frac{1}{2} \left( \frac{dx'}{d\tau'} \right)^2 + \frac{1}{2} \kappa x'^2 + v(x') \quad (17)$$

respectively.

We will call the  $(x', \tau')$  coordinate system the local frame and  $(x, \tau)$  the global frame. From the equation of motion for  $x'$  given by Eq. (16), it can be seen that in the local frame (for the case  $u = 0$ ) the scalar, linear, and quadratic portions of the potential proportional to  $g_1$ ,  $g_2$ , and  $g_3$  drop out and that only the potential  $v(x')$ , which can be thought of as being centered about the time varying position of its minimum  $x_{\min} = \sigma(\tau)$ , affects the particle motion. The local coordinate  $x'$  is thus simply related to the original global coordinate  $x$  by a time varying shift  $\sigma(\tau)$  (which locates a potential extremum or minimum) and a time varying scale factor  $\rho(\tau)$ .

The expression for the Ermakov invariant in terms of local variables given by Eq. (17) appears in the form of a total (local) energy that is conserved. It should not be confused with the total energy of the system given by

$$E(\tau) = \frac{1}{2} \left( \frac{dx}{d\tau} \right)^2 + V_I(x, \tau) \quad (18)$$

which is time varying.

For the wave equation the Ermakov invariant becomes an operator with the replacements

$$\frac{dx}{d\tau} \rightarrow p = -i \frac{\partial}{\partial x} \quad (19)$$

and

$$\frac{dx'}{d\tau'} \rightarrow p' = -i \frac{\partial}{\partial x'} \quad (20)$$

The respective invariants

$$I'_{op} = -\frac{1}{2} \frac{\partial^2}{\partial x'^2} + \frac{1}{2} \kappa x'^2 + v(x') \quad (21)$$

and

$$I_{op} = \frac{1}{2} \left[ \left( \rho p - \dot{\rho} x \right) - \left( \sigma p' - \dot{\sigma} x' \right) \right]^2 + \frac{\kappa}{2} \left( \frac{x - \sigma}{\rho} \right) + v \left( \frac{x - \sigma}{\rho} \right) \quad (22)$$

are related by a unitary transformation<sup>2</sup>

$$I_{op} = e^{i\Phi} I'_{op} e^{-i\Phi} \quad (23)$$

where

$$\Phi = \frac{\dot{p}}{\rho} \left( \frac{x^2}{2} + x \right) - \dot{\sigma} x. \quad (24)$$

By using the constraint Eqs. (10) and (11), it can be shown that both  $I_{op}$  and  $I$  are truly invariant, that is,

$$\frac{d}{dt} I_{op} = \frac{1}{i} [I_{op}, H] + \frac{\partial}{\partial t} I_{op} \quad (25)$$

and

$$\frac{d}{dt} I = 0. \quad (26)$$

### 3. A MORSE POTENTIAL MODEL FOR THE E-F LAYER TROUGH

In order to apply Ermakov invariant theory to the ionospheric ray tracing problem, the ionospheric potential function  $V_I(x, \tau)$  given by Eq. (7) must be cast into the form of the time dependent function  $V_E(x, \tau)$  given by Eq. (9). Neglecting for the moment the presence of an  $F_1$  layer, an effective ionospheric potential will resemble the double-well potential  $V_{CH}(x, \tau)$  shown in Figure 1 that was formed by superposing E and  $F_2$  layers approximated by the Chapman function

$$f_{CH}(x) = e^{1/2(1 - x - e^{-x})}. \quad (27)$$

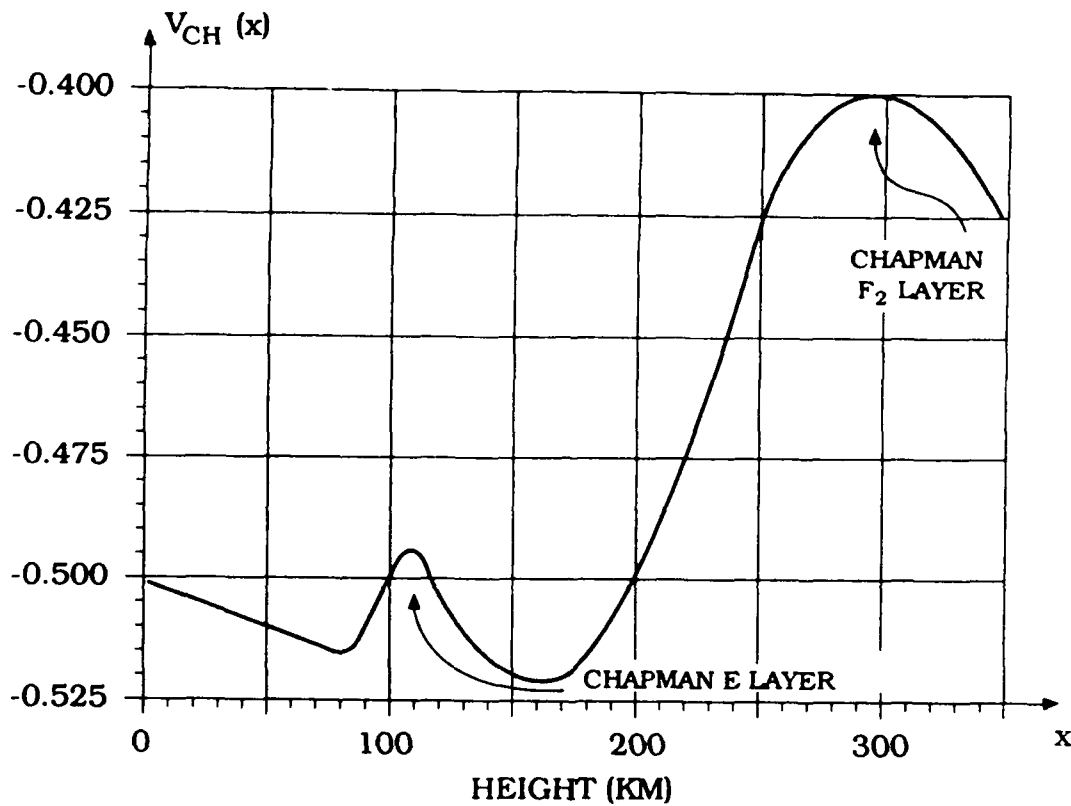


Figure 1. Plot of the Effective Ionospheric Potential  $V_{CH}(x)$  as a Function of Height  $x$ .

In terms of the layer half-widths  $y_e(z)$ ,  $y_f(z)$  heights  $x_e(z)$ ,  $x_f(z)$  and frequencies  $\nu_e(z)$ ,  $\nu_f(z)$  (provided by IONCAP)<sup>3</sup> this effective ionospheric potential including the curvature term is written as

$$V_{ICH}(x, \tau) = -\frac{1}{2} \left( 1 + 2x/R_0 \right) + \frac{\nu_e^2}{2\nu^2} f_{CH} \left( \frac{x - x_e}{y_e} \right) + \frac{\nu_f^2}{2\nu^2} f_{CH} \left( \frac{x - x_f}{y_f} \right). \quad (28)$$

Finding a potential function approximating  $V_{CH}(x, \tau)$  with known analytic solutions and separately adjustable well parameters would seem to be a remote possibility. If the requirement of separately adjustable well parameters is relaxed, it is, however, quite possible

that very good approximations to the potential of Figure 1 could be found by employing the Darboux transformation.<sup>5</sup> The effect of the Darboux transformation given by

$$\tilde{V}(x) = \phi_0(x) \frac{d^2}{dx^2} \left( \frac{1}{\phi_0(x)} \right) \quad (29)$$

$$\tilde{\psi}(x) = \frac{d\phi}{dx} - \frac{d\phi_0}{dx} \frac{\phi(x)}{\phi_0(x)} \quad (30)$$

is to transform a single-well potential  $V(x)$  with known solution  $\phi(x)$  into a generally non-symmetric double-well potential  $\tilde{V}$  with solution  $\tilde{\psi}$ . By its construction, however, the Darboux transform does not allow either well to vary independently of the other, thus limiting its usefulness for ionospheric ray tracing where the ground-E layer and E-F<sub>2</sub> layer potential wells do vary independently.

In order to insure independent variation of the potential wells (brought about by the independent variation of the constitutive ionospheric layers), it is thus necessary to piece together truncated wells or layers along common boundaries. In this section we will look at an example of approximating the ionospheric potential by piecing together two potential wells truncated at  $x_e$ , the position of the E-layer peak; while in Section 5 we discuss approximating the ionospheric potential by piecing together either inverted Morse potentials or parabolic layers connected by straight line segments.

While piecing together two truncated potentials leads to difficulties in generating solutions to the wave [Eq. (6)] for states near the top of the barrier separating the two wells due to tunneling and mixing, these difficulties do not exist for solutions to the equation of motion [Eq. (12)] describing ray trajectories.

The steps for ionospheric ray tracing employing the results of Ermakov invariant theory for potential wells formed by joining together separate soluble sectors are the following:

- 1) Choose a form  $V_E(x, \tau)$  [Eq. (9)] that can closely approximate the ionospheric potential  $V_1(x, \tau)$  [Eq. (7)] over its entire range by varying the scale, shift and level functions  $\rho(\tau)$ ,  $\sigma(\tau)$ , and  $g_0(\tau)$  appropriate to each sector with  $g_1(\tau)$ , and  $g_2(\tau)$ , set to zero.
- 2) On the scale of a wavelength of the propagating wave,  $\ddot{\sigma}$  and  $\ddot{\rho}$  are assumed to be negligible. For a given great circle path  $\rho(\tau)$ ,  $\sigma(\tau)$ , and  $g_0(\tau)$  appropriate to each sector can thus be approximated by fitting  $V_E(x, \tau)$  to  $V_1(x, \tau)$  for each range point  $\tau_i$ .
- 3) Launching a ray at some point  $(x, \tau_0)$  in  $V_E(x, \tau)$  at a given incidence angle and frequency determines the Ermakov invariant  $I$  for that potential sector and, assuming the solution to the

---

<sup>5</sup> Zheng, W.M. (1984) The Darboux Transformation and Solvable Double-Well Potential Models for Schroedinger Equations, *J. Math. Phys.*, **25**:88.



equation of motion [Eq. (16)] (with  $\kappa = 0$ ) is known, the ray path is determined up to the point where the ray crosses a boundary into another sector of the potential.

4) At a boundary crossing using the known  $x$ ,  $\dot{x}$ ,  $\sigma$ ,  $\rho$ ,  $\dot{\sigma}$ , and  $\dot{\rho}$ , the Ermakov invariant is calculated for the new sector of the potential and motion in this sector is determined as in step 3. Any rays that hit the ground at  $x = 0$  are assumed to be perfectly reflected.

5) The final ray path  $x(\tau)$ , is found by inverting Eqs. (14) and (15) and piecing the ray paths in the various sectors together.

Instead of treating the entire ionospheric potential at once, we shall first focus on the potential well formed by the E and F<sub>2</sub> layers and the propagation of rays in this E-F<sub>2</sub> duct. From the graph of  $V_{CH}(x, z)$  in Figure 1 it can be seen that the E-F<sub>2</sub> potential is asymmetric, with a slope that is steeper above the minimum than below it. A soluble potential that can be adjusted to fit the E-F<sub>2</sub> is the Morse potential given by

$$V_M(x') = \gamma^2 (e^{\alpha x'} - 1)^2 \quad (31)$$

and plotted in Figure 2.

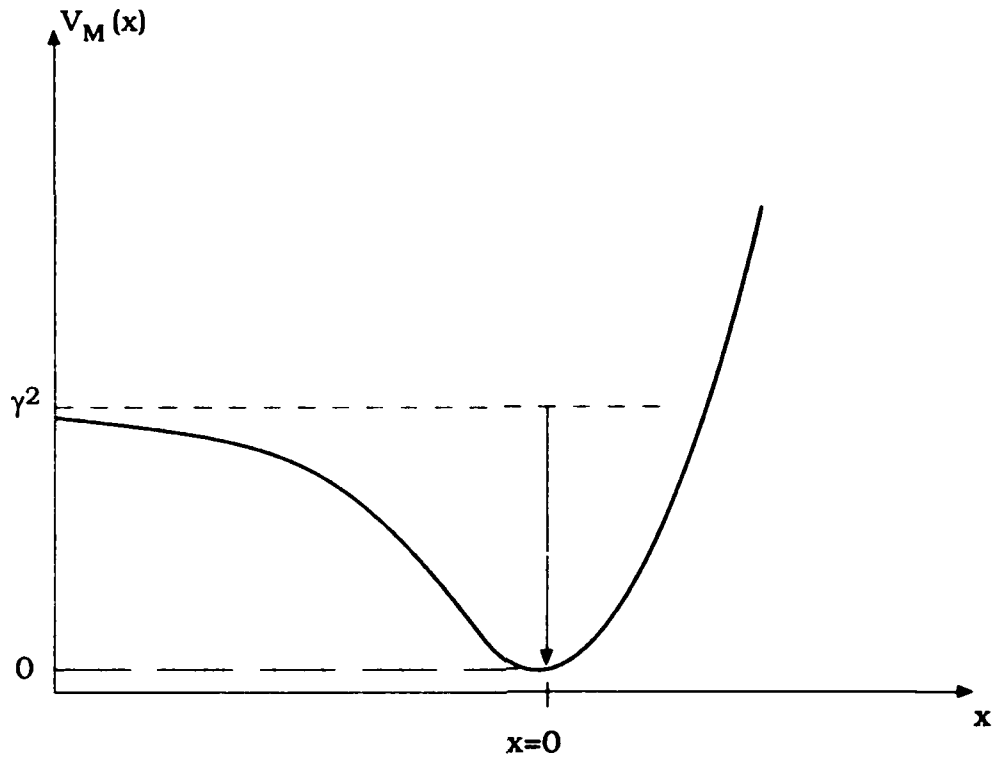


Figure 2. Plot of the Morse Potential  $V_M(x) = \gamma^2 (e^{\alpha x} - 1)^2$  as a Function of Height  $x$  with  $\gamma^2 = 1$  and  $\alpha = 1$ .

For  $E' < \gamma^2$  the solution for ray paths are given by<sup>6</sup>

$$e^{-\alpha x'} = x_{CO} - A(E') \cos(\omega_C(E') \tau') \quad (32)$$

where

$$x_{CO} = \gamma^2 / (\gamma^2 - E') \quad (33)$$

<sup>6</sup> Nieto, M.M., Simmons, L.M. (1979) Coherent States for General Potentials III. Non-confining One-Dimensional Examples, *Phys. Rev. D*, **20**:1342.

$$A(E') = (\gamma^2 \cdot E')^{1/2} / (\gamma^2 - E') \quad (34)$$

and

$$\omega_c(E') = [2\alpha^2 (\gamma^2 - E')]^{1/2}. \quad (35)$$

For  $E' > \gamma^2$  the solutions are given by the same expression with  $\omega_b = |\omega_c|$  replacing  $\omega_c$  and cosh replacing cos.

While the main purpose of this section is to model and examine the motion of rays in the E-F<sub>2</sub> duct, a simplified ground E-layer potential will be added on in order to have a rough model available for launching rays from a ground transmitter. The ground E-layer potential will thus be approximated by a simple linear potential with slope  $g = 1/R_0$  from  $V_m = -\frac{1}{2}$  at  $x = 0$  to  $V_M = -(1 + \sigma_L/R_0)$  at the minimum  $x = \sigma_L$  and a positive slope  $g = g_r$  for  $\sigma_L \leq x < x_e$ . The right side of this potential will be constrained to equal the value of  $V_{CH}(x_e)$  at  $x = x_e$ , thus, the position of the minimum  $\sigma_L(\tau_1)$  is determined by the intersection of the right and left sides of the potential and will move lower (higher) as the value of  $V_{CH}(x_e)$  increases (decreases). The general solution for a ray in this potential is given by

$$x' = \frac{1}{2} g \tau'^2 + v_0 \tau' + x'_0 \quad (36)$$

where

$$g = \begin{cases} -1/R_0 & x' < 0 \\ g_r & x' \geq 0 \end{cases} \quad (37)$$

To cast the E-F<sub>2</sub> potential well into the Ermakov form, the Morse potential is fit at each range point  $\tau_1$  by a least squares approximation. It is assumed that  $g_1(\tau)$ ,  $g_2(\tau)$ , and  $n$  are zero. At the initial range point,  $\alpha$  and  $\gamma^2$  are determined by least squares fit with  $\rho(0) = 1$ ,  $g_0(0) = 0$  and  $\sigma(0) = x_{min}$ . At subsequent range points,  $\sigma(\tau_1)$ ,  $\rho(\tau_1)$ , and  $g_0(\tau_1)$  are fit by minimizing

$$\int_{x_1}^{x_r} \left[ V_{1CH}(x, \tau_1) - \gamma^2 (e^{\alpha[x - \sigma(\tau_1)] / \rho(\tau_1)} - 1)^2 / \rho(\tau_1)^2 - g_0(\tau_1) \right]^2 dx \quad (38)$$

where  $x_1$  and  $x_r$  bound the E-F<sub>2</sub> potential as described Reference 7.

Having determined the parameters  $\alpha$ ,  $\gamma^2$ , and the set of values for  $\{\sigma(\tau_i)\}$  and  $\{\rho(\tau_i)\}$ , the path for a ray launched in the E-F<sub>2</sub> duct at some arbitrary point (at  $x = x_e$  if it arrived by passing over the E-layer peak) will be given for all subsequent range values by Eq. (32) until it leaves the duct, either by passing over the E-layer peak at  $x = x_e$  or at an analagous point  $x = x_f$  which is taken as representing the F-layer peak. The Ermakov invariant  $I_M$  determined by the values of the quantities  $x$ ,  $\rho$ , and  $\ddot{\sigma}$ , the potential  $V_M [(x - \sigma) / \rho]$  and the first derivatives  $\dot{x}$ ,  $\dot{\rho}$ , and  $\dot{\sigma}$  at the launch point, can then be used to determine the velocity at the exit point as

$$\dot{x} = \frac{dx'}{d\tau'} / \rho + \dot{\sigma} + \dot{\rho} x' \quad (39)$$

where  $dx'/dt'$  is related to  $I_M$  by

$$I_M = E' = \left( \frac{dx'}{d\tau'} \right)^2 + V_M(x'). \quad (40)$$

If the ray crosses over into the ground-E potential well, the new invariant

$$I_G = \frac{\dot{x}^2}{2} + [x(\tau_b) - \sigma_M(\tau_b)] \cdot g_r \quad (41)$$

with  $\tau_b$  the range at the boundary crossing, is conserved as long as the ray propagates in the ground E-layer potential. If we were able to treat the ionospheric double-well potential exactly in the Ermakov formalism, there would be only one invariant. As we have divided the potential into sectors, there will be an Ermakov invariant connected with propagation in each sector and crossing from one to the other will entail a new calculation of the sector just entered. Since  $\rho$  and  $\sigma$  for the Morse potential can change independently of  $\rho$  ( $= 1$ ) and  $\sigma$  for the ground E-layer potential, there is no necessity for  $I_M(\tau_1)$  to equal  $I_M(\tau_2)$  if the ray has propagated in the ground E-layer potential at some range between  $\tau_2$  and  $\tau_1$ . A similar statement holds true for  $I_G$ .

The details of numerical fitting the Morse potential wells and plotting ray paths are discussed in Reference 7. We note that since both the E and F<sub>2</sub> layer peaks have been approximated by functions that have non-parabolic slopes at  $x_e$  and  $x_f$ , there will be no Pedersen high rays.

#### 4. COHERENT STATES AND RAY PATHS FOR THE MORSE POTENTIAL

While the discussion in Section 3 was concerned with determining solutions of the classical equations of motion for ray paths, the same time-dependent theory can be applied to solutions of the wave [Eq. (6)] if the operator form for the Ermakov invariants, Eq. (22) or (23) is used. Dhara and Lawande<sup>8</sup> have shown that the Feynman propagator for a time-dependent system that obeys the constraint conditions [Eq. (10) and (11)] may be written as

$$K_0(x_b, \tau_b; x_a, \tau_a) = (\rho_a \rho_b)^{-1/2} e^{ik_0(x_b - x_a)} \bar{K}_0(x'_b, \tau'_b; x'_a, \tau'_a) \quad (42)$$

where  $\bar{K}_0$  is the propagator in the local potential  $v(x')$

$$\bar{K}_0(x'_b, \tau'_b; x'_a, \tau'_a) = \sum_n \left[ e^{-i E'_n \int_{\tau_a}^{\tau_b} \frac{d\tau}{\rho^2(\tau)}} \right] \phi_n \left( \frac{x'_b - \sigma(\tau'_b)}{\rho(\tau'_b)} \right) \phi_n \left( \frac{x'_a - \sigma(\tau'_a)}{\rho(\tau'_a)} \right) \quad (43)$$

and where  $E'_n$  are the eigenvalues of  $I'_{op}$  with

$$x = \frac{\dot{\rho} x^2}{2\rho} + x(\dot{\sigma} - \sigma \dot{\rho}/\rho) - \frac{1}{2} \int_0^\tau \rho^2(\tau') \frac{d}{d\tau'} (\sigma/\rho)^2 d\tau'. \quad (44)$$

Since

<sup>7</sup> Yukon, S.P. (1986) Calculation of Ray Paths in the Ionosphere Using an Analytic Ray Tracing Technique, RADC-TR-86-125, ADA178888.

<sup>8</sup> Dhara, A.K., and Lawande, S.V. (1984) Feynman Propagators for Time Dependent Lagrangians Possessing an Invariant Quadratic in Momentum, *J. Phys. A*, 17:2423.

$$\psi(x_b, \tau_b) = \int dx_a K_0(x_b, \tau_b; x_a, \tau_a) \psi(x_a, \tau_a). \quad (45)$$

The propagator of Eq. (43) projects the wave function  $\psi(x_a, \tau_a)$  into a sum of 'local' eigenfunctions  $\phi_n\left(\frac{(x-\sigma)}{\rho}\right)$  each of which has its phase increased according to its 'local' energy eigenvalue  $E'_n$  times the local time

$$\tau' = \int^{\tau} \frac{d\tau''}{\rho^2(\tau'')}. \quad (46)$$

If an appropriate soluble double-well potential could be found that would model the ionospheric potential ( $F_1$  layer neglected), then the above propagator would convey all of the information necessary for mapping and for wave propagation. Since it is extremely difficult to find a soluble double-well potential that can model a time-path-dependent ionosphere, a practical measure is to piece together truncated soluble single-well potentials as outlined in Section 3. The resulting total wave function can be approximated by appropriate superpositions of wave functions belonging to each well. If eigenfunctions and eigenvalues can be found for each truncated well separately, the combined potential wells may be described by the same formalism that is used for treating coupled optical waveguides.<sup>9</sup>

If we can confine our attention to low lying states in each of the potential wells separately, the details of how the potentials are truncated should not greatly affect these states. For low lying states in the  $E$ - $F_2$  potential that can be described by the Morse potential [Eq. (31)] the eigenvalues and eigenfunctions are given by<sup>10</sup>

$$E_n = E_0 \left[ 2\lambda \left( n + \frac{1}{2} \right) - \left( n + \frac{1}{2} \right)^2 \right] \quad (47)$$

with

<sup>9</sup> Marcuse, D. (1974) *Theory of Dielectric Optical Waveguides*, Academic Press, New York.

<sup>10</sup> Morse, P.M. (1929) Diatomic Molecules According to the Wave Mechanics II. Vibrational Levels, *Phys. Rev.*, **34**:57.

$$E_0 = \hbar^2 \alpha^2 / 2m, \lambda^2 = \gamma^2 / E_0 \quad (48)$$

and

$$\phi_n = N(n, \lambda) \phi_n^0(y) \quad (49)$$

$$= \left[ \frac{\alpha (2\lambda - 2n - 1)}{\Gamma(2\lambda - n)} \Gamma(n + 1) \right]^{1/2} y^{(\lambda - 1/2 - n)} e^{-y/2} L_n^{(2\lambda - 2n - 1)}(y)$$

with

$$y = 2\lambda e^{-\alpha x} \quad (50)$$

where  $L_n^{(\mu)}$  is a generalized Laguerre polynomial.

#### 4.1 Coherent States of the Morse Potential

It has been pointed out by Schrodinger<sup>11</sup> and subsequently by several other authors<sup>12</sup> that for wave packets formed to minimize the position-momentum uncertainty for a harmonic oscillator, the expectation value  $\langle x(\tau) \rangle$  will follow the classical motion of an harmonic oscillator. Subsequent authors have generalized such minimum uncertainty states to coherent states that can be defined either as eigenstates of the annihilation operator

$$a = \left( p + \frac{m\omega}{i} x \right) / \sqrt{2m\omega} \quad (51)$$

<sup>11</sup> Schrodinger, E. (1926) *Naturwissenschaften*, 14:664, English translation in Schrodinger, E. (1928) *Collected Papers on Wave Mechanics*, p. 41, Blackie & Son, London.

<sup>12</sup> Nieto, M.M., Simmons Jr., L.M. (1979) Coherent States for General Potentials, I. Formalism, *Phys. Rev.*, D20:1321.

such that  $a|\alpha\rangle = \alpha|\alpha\rangle$ , or as a displacement by  $\alpha$  of the ground state  $|0\rangle$ .

For the harmonic oscillator the two definitions are equivalent due to the special circumstance that the oscillator frequency is independent of energy, with eigenenergies equally spaced. For the Morse potential these conditions do not hold as can be seen from the expression for the frequency [Eq. (35)] which is energy dependent and from the expression [Eq. (47)] for  $E_n$  which depends on  $n^2$ .

By treating

$$X_c = e^{-\alpha x} - \frac{\gamma^2}{(\gamma^2 - E)} = A(E) \sin[\omega_c(E) \tau] \quad (52)$$

and

$$P_c = \alpha P e^{-\alpha x} = m \omega_c(E) \cos[\omega_c(E) \tau] \quad (53)$$

as an appropriate pair of classical (but not canonical) variables for the problem, since their classical equations of motion are the same as the harmonic oscillator, Nieto<sup>12</sup> formed minimum-uncertainty coherent states that minimize  $\langle \Delta X_c \rangle \langle \Delta P_c \rangle$ . In tracing out this subsequent time evolution of these states it was found that after a few cycles the wave packets would tend to break up and disperse. More recently Gerry<sup>13</sup> has shown that the Morse oscillator may be treated as an harmonic oscillator evolving in a curved phase space with a transformed time parameter

$$\tau = \int_0^t dt' e^{-\alpha x(t')}. \quad (54)$$

The coherent states can thus be formed as minimum uncertainty states in the transformed harmonic oscillator representation. When projected back into original variables,  $\langle x(\tau) \rangle$  for these coherent states should follow the classical path for a Morse oscillator.

---

<sup>13</sup> Gerry, C.C. (1986) Coherent States and a Path Integral for the Morse Oscillator, *Phys. Rev.*, **A33**:2207.



## 4.2 Focusing Properties of the Morse Potential

It has been noted for many years<sup>14</sup> that underwater sound channels exist in the oceans that can play the same role for acoustic waves as ionospheric ducts do for HF electromagnetic waves.<sup>15</sup> In the underwater sound case there exists a focusing phenomenon shown in Figure 3 wherein rays launched from a source near the sound axis will be repeatedly focused as they travel downrange in the sound channel. The regions where this quasi-focusing occurs are called convergence zones. The sound speed profile for underwater sound channels is well-approximated by the Munk profile<sup>16</sup>

$$\frac{c(x) - c_0}{c_0} = 2 [e^\eta - \eta - 1], \quad \eta = x - x_0 \quad (55)$$

shown in Figure 3. Near the origin the Munk profile can be seen to be quite similar to the Morse potential for small  $\eta$ . Writing the Morse potential as

$$V_M = \gamma^2 (e^\eta - 2e^{\eta/2} + 1) \quad (56)$$

and expanding only the second term to first order, that is

$$-2e^{\eta/2} \approx -2 - \eta \quad (57)$$

yields an expression which is identical to the Munk profile. Repeated focusing could therefore be expected to occur in the case of ducted ionospheric propagation described by the Morse potential.

<sup>14</sup> Ewing, W.M., Worzel, J.L. (1948) Long Range Sound Transmission, *Geol. Soc. Am. Mem.*, 27, Part III, 1.

<sup>15</sup> Quäck, E. (1927) Propagation of Short Waves Around the Earth, *Proc. IRE*, 15:341. Further references in Toman, K. (1979) High-Frequency Ionospheric Ducting - A Review, *Radio Science*, 14:447.

<sup>16</sup> Brekhouskikh, L. and Lyzanov, Yu (1982) *Fundamentals of Ocean Acoustics*, Springer-Verlag, Berlin, Heidelberg, New York, p. 118.

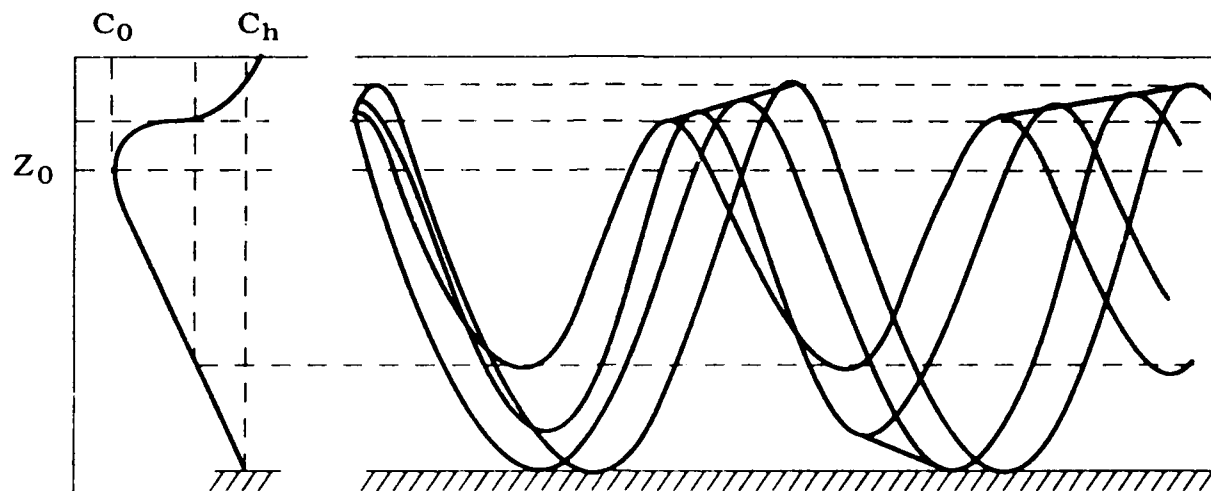


Figure 3. Plot of the Munk Profile and Ray Convergence Zones from Reference 16.

As it turns out, repeated focusing in the Morse potential can be exact, that is real point focusing as opposed to progressively wider convergence zones. To see this we first note that to have repeated focusing, the propagation constants  $\beta_n$  must satisfy

$$\beta_n - \beta_{n'} = I_{nn'} \frac{2\pi}{L} \quad (58)$$

where  $I_{nn'}$  is an arbitrary integer function and  $L$  is the focal length.<sup>17</sup> There exist families of refraction index profiles that are finite at spatial infinity and have the focusing property described by Eq. (58), for example

$$V_f(x) = \text{sech}^2(\Lambda(x - x_0)) \quad \text{where} \quad \beta_n = n \cdot k_0. \quad (59)$$

For the Morse potential, which does not fit this category since  $V_M(x)$  is unbounded as  $x \rightarrow +\infty$ , it is still possible to satisfy the focusing condition [Eq. (58)] due to the presence of the

<sup>17</sup> Yukon, S.P. and Bendow, B. (1980) Design of Waveguides with Prescribed Propagation Constants, *J. Opt. Soc. Am.*, 70:172.

$(n + 1/2)^2$  term in the expression for the energy eigenvalue given in Eq. (47). In order to satisfy condition  $I_{nn} = 1$ ,  $\beta_n$  can be written as

$$\beta_n = p + q \cdot n. \quad (60)$$

This relation will then hold if  $\gamma^2 = n_0^2/2$ , where  $n_0^2/2$  is the magnitude of the potential well minimum. From the ionospheric paths that so far have been fitted by the Morse potential it appears that this condition can be met, but only for frequencies in the range of 6–10 MHz.

Since only a portion of the E–F<sub>2</sub> ionospheric duct can be modeled by the Morse potential, repeated focusing cannot be expected to hold for weakly bound ducted modes, but should apply to the tightly bound modes. From the correspondence between rays and coherent states discussed in the previous section it is expected that repeated focusing will thus hold for low angle ducted rays.

It can also be seen that repeated focusing will be an invariant property of an ionospheric duct; if repeated focusing holds true in the local frame, a somewhat distorted repeated focusing will hold in the global frame. Thus, rays leaving an initial point

$$x_0 = \sigma(\tau_0) + x'_0 \cdot \rho(\tau_0) \quad (61)$$

at range  $\tau_0$  will refocus at

$$x_1 = \sigma(\tau_1) + x'_1 \cdot \rho(\tau_1) \quad (62)$$

at range  $\tau_1$ , where  $\tau_0$  and  $\tau_1$  are related by

$$L = \int_{\tau_0}^{\tau_1} \frac{dt}{\rho^2(t)} \quad (63)$$

providing the differential constraint conditions [Eq. (10) and Eq. (11)] are satisfied. In the global frame the focal length is a function of  $\rho(\tau)$ , and the mapping of an interval  $a \leq x \leq b$  will be displaced by  $\sigma(\tau_1) - \sigma(\tau_0)$  and enlarged or reduced depending on whether  $\rho(\tau_1)$  is greater than or less than  $\rho(\tau_2)$ .

## 5. RAY TRACING IN THE IONCAP IONOSPHERE

The ionospheric electron density profiles provided by the IONCAP program<sup>3</sup> consist of E, F<sub>2</sub> and an optional F<sub>1</sub> layers, joined together by straight line segments. The parabolic layers are described by the plasma frequency

$$v_p^2(x) = v_0^2 \left[ 1 - (x - x_0)^2 / y_0^2 \right] \quad (64)$$

where  $v_0$ ,  $x_0$ , and  $y_0$  are the peak plasma frequency, layer height and half width respectively with the refractive index  $\epsilon(x) = n^2(x)$  related to  $v_p^2(x)$  by

$$\epsilon(x) = 1 - v_p^2(x) / v^2. \quad (65)$$

The base of the E-layer is set at  $h_1 = 90$  km. The straight line that models the valley between the E- and F<sub>2</sub>- layers, starts at a point  $h_2$  where the plasma frequency is  $0.8516 f_{0E}$  and ends at a point  $h_3$  where the plasma frequency is  $0.98 f_{0E}$ . This yields

$$\begin{aligned} h_2 &= x_{0E} + y_{0E} \sqrt{1 - (.8516)^2} \\ &= 120.48 \text{ km} \end{aligned} \quad (66)$$

and

$$h_3 = x_{0F_2} - y_{0F_2} \sqrt{1 - (.98 f_{0E} / f_{0F_2})^2}. \quad (67)$$

The effective ionospheric potential is that given by the sum of curvature correction term

$$\delta V_E = -\frac{\beta^2}{2} \left( + \frac{2x}{R_0} - \frac{3}{2} \frac{x^2}{R_0^2} \right) \quad (68)$$

and

$$V_E^0 = -\frac{1}{2} (n^2(x, \tau) + \beta^2) \quad (69)$$

where  $\beta = \cos(\theta)$ , with  $\theta$  the launch angle with respect to the horizontal direction. The resulting potential well is shown in Figure 4. If the ionospheric potential is thought of as two separate wells joined at the E-layer peak as in the case of the Morse oscillator model of Section 3, each separate well is then composed of parabolic and linear pieces, and would not be in the class of potentials soluble by Ermakov theory since the shape of the well cannot be expressed as a single function  $V[(x - \sigma) / \rho]$ .

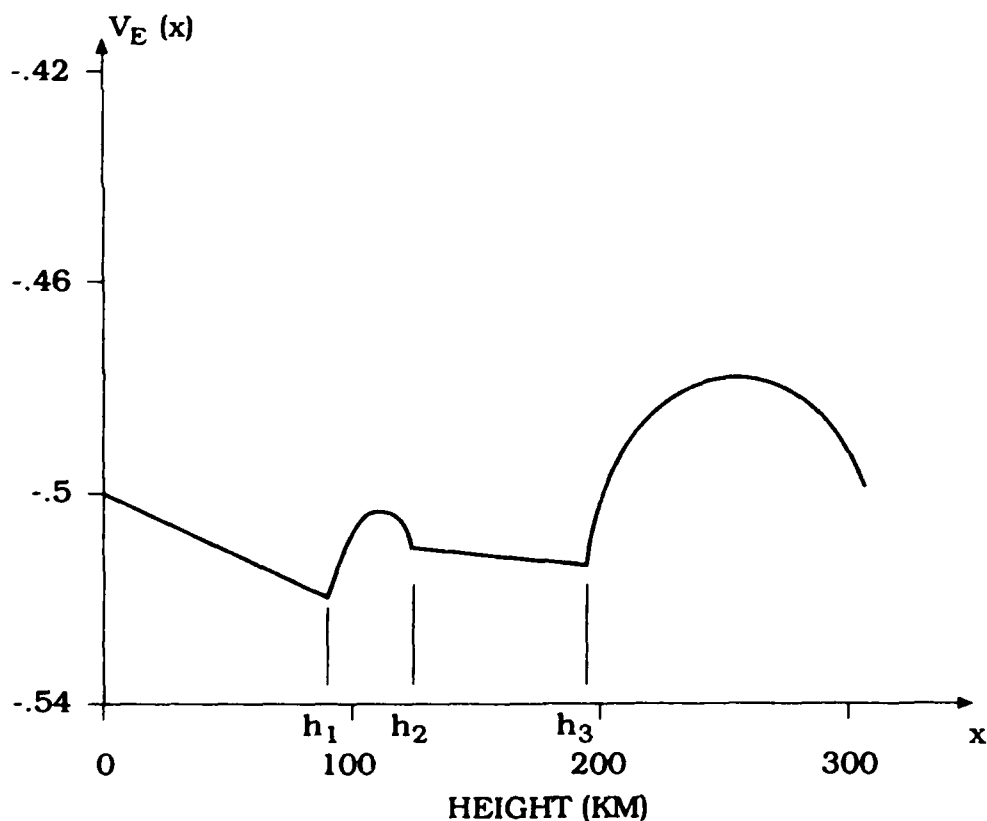


Figure 4. Plot of the IONCAP Effective Ionospheric Potential  $V_E(x)$  as a Function of Height  $x$ .

If, however, the ionospheric potential is broken up into sectors as shown in Figure 5, Ermakov theory may then be applied to each of the four potentials. The potentials in Sectors II and IV are not what one usually thinks of as potentials since they have no local minimum, but they are valid potentials for Ermakov theory and have recently been shown<sup>18</sup> to have coherent states that follow the classical motion. For an inverted parabola centered about  $x = 0$  the classical solutions are

$$x(\tau) = x_0 \cos(\omega \tau) + p_0 \sin(\omega \tau) \quad (70)$$

$$\text{for } E = 1/2 (p_0^2 - x_0^2) \leq 0$$

and

$$x(\tau) = x_0 \text{ch}(\omega \tau) + p_0 \text{sh}(\omega \tau) \quad (71)$$

$$\text{for } E > 0.$$

---

<sup>18</sup> Barton, G. (1986) Quantum Mechanics of the Inverted Oscillator Potential, *Ann. of Phys.*, **166**:322.

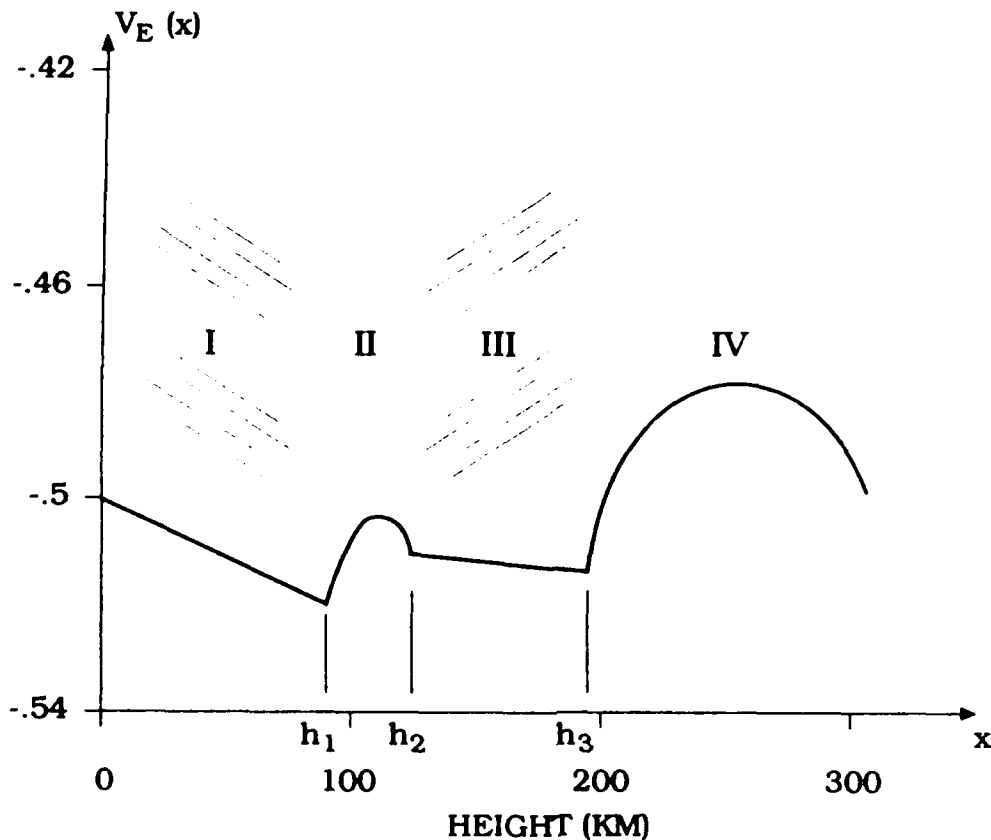


Figure 5. The IONCAP Potential of Figure 4 Broken up into Sector Potential Wells I through IV.

Since  $v_0$ ,  $x_0$ , and  $y_0$  are provided by IONCAP at each range point,  $\sigma(z)$ , and  $\rho(z)$  can be found algebraically and need not be determined by the fitting procedure that was necessary for the Morse potential. The tradeoff for not having to fit the parameters  $\sigma(z)$ , and  $\rho(z)$  is that there are now more boundary crossings (three vs one for the Morse case) where the portion of the range step that is in each sector must be determined; for example for  $x(z_i)$  in region III and  $x(z_i + 1)$  in region IV it is necessary to find  $z_b$  such that  $x(z_b) = h_3(z_b)$ . Determining  $z_b$  is straightforward for the above example (complicated somewhat by the fact that the  $h_3$  boundary is a function of range), if the ray did not reverse direction between  $z_i$  and  $z_i + 1$ . If there is a velocity reversal in this interval then three possible cases must be considered as depicted in Figure 6 below.

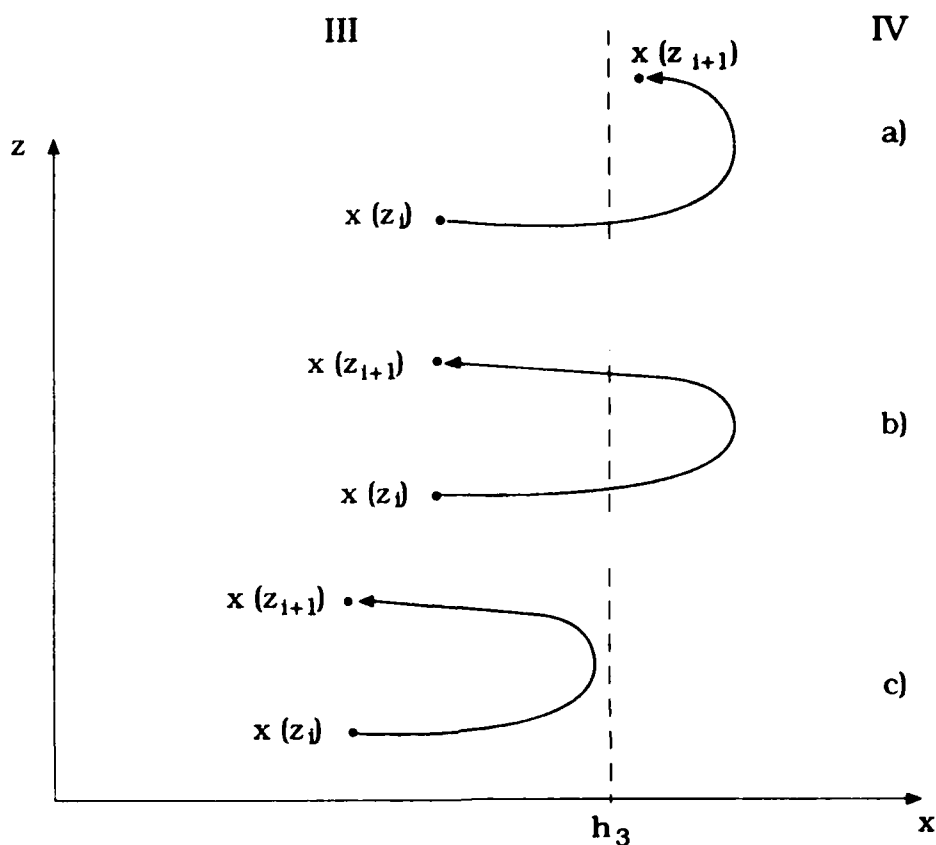


Figure 6. Three Possible Cases for Turning Point Behavior Near a Sector Boundary.

To distinguish between them it is thus necessary to calculate the turning point.

One further situation where care must be exercised is for rays that cross very near the peak of the nighttime E-layer. The peak of the parabola representing the E-layer electron density will, upon being added to the curvature term to form the effective potential, be shifted to a lower altitude by an amount

$$l_e = -\frac{y_{0E}^2}{2R_0} \left( \frac{v}{v_e} \right)^2 \quad (72)$$

as well as being shifted down in magnitude by an amount



$$\mu_e = -\frac{x_e}{R_0} + \frac{y_{0E}^2}{4R_0^2} \left( \frac{y}{v_e} \right)^2. \quad (73)$$

It is possible for the potential peak to be shifted down (in altitude) so far that the effective potential between  $h_1$  and  $h_2$  is the mapping of a topside segment of the inverted parabolic potential and does not contain the peak. A ray that crosses from  $x < h_1$  to  $x > h_1$  may then find itself on the topside region of an inverted parabolic potential even though its energy is negative with respect to the shifted peak. While unexpected, such behavior is easily dealt with simply by checking whether

$$h'_1 = (h_1 - \sigma(\tau_b)) / \rho(\tau_b) \quad (74)$$

is greater than or less than zero. For  $h'_1 < 0$  the E layer boundary is still left of the peak in local coordinates, while for  $h'_1 > 0$  the ray is on the topside of an inverted parabolic potential.

The testing to determine initial conditions occurs only for range steps where the ray crosses a boundary. Thus given the ionospheric parameters for a given great circle path from IONCAP, tracing rays employing Ermakov invariants essentially amounts to joining up the analytic solutions in each sector. The only real numerical work involved is in the calculation of the fractional range step remainders in crossing sector boundaries. For an around-the-world path there can be on the order of 20 complete oscillations in the EF potential well which would require 40 numerical minimizations to determine the range step remainders. These may be accomplished very efficiently using standard Newton's minimization methods so that a complete round-the-world ray trace may be carried out in approximately one-half second. An ionogram for the same path covering angles from  $0^\circ$  to  $40^\circ$  in one-half degree steps and the even frequencies from 6 to 30 MHz takes approximately 3 minutes to calculate.

The  $F_1$  layer as modeled by IONCAP may also be straightforwardly included in the ray tracing code as a third parabolic (or linear) layer centered at the  $F_1$  layer height. This will entail the calculation of one more boundary crossing for motion between the E and  $F_2$  layers. Since a ray may become trapped between the  $F_1$  and  $F_2$  boundary, the same checking for one-step ray reversals at the  $F_1$ - $F_2$  boundary must be carried out as was done for the case of the III- $F_2$  boundary described above. Thus an approximate 10 percent-30 percent increase in computation time could be expected by turning on the  $F_1$  layer.

Some examples of ray tracings and ionograms made using the methods outlined above are shown in Figures 7 through 11 along with results obtained using the Jones-Stephenson program for the same IONCAP parameters.

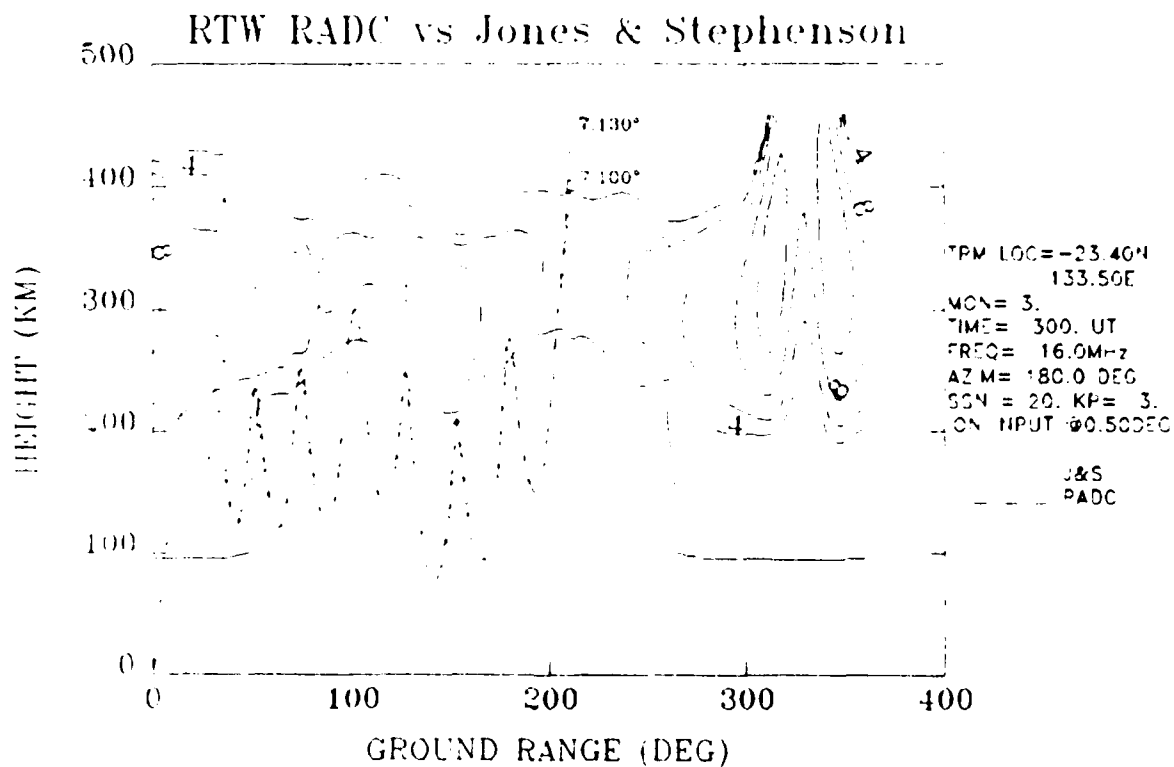


**Figure 7. Ray Traces Using Current Model vs Jones-Stephenson's<sup>1</sup> Program for Frequency = 16 MHz, Takeoff Angle = 7.1°.**

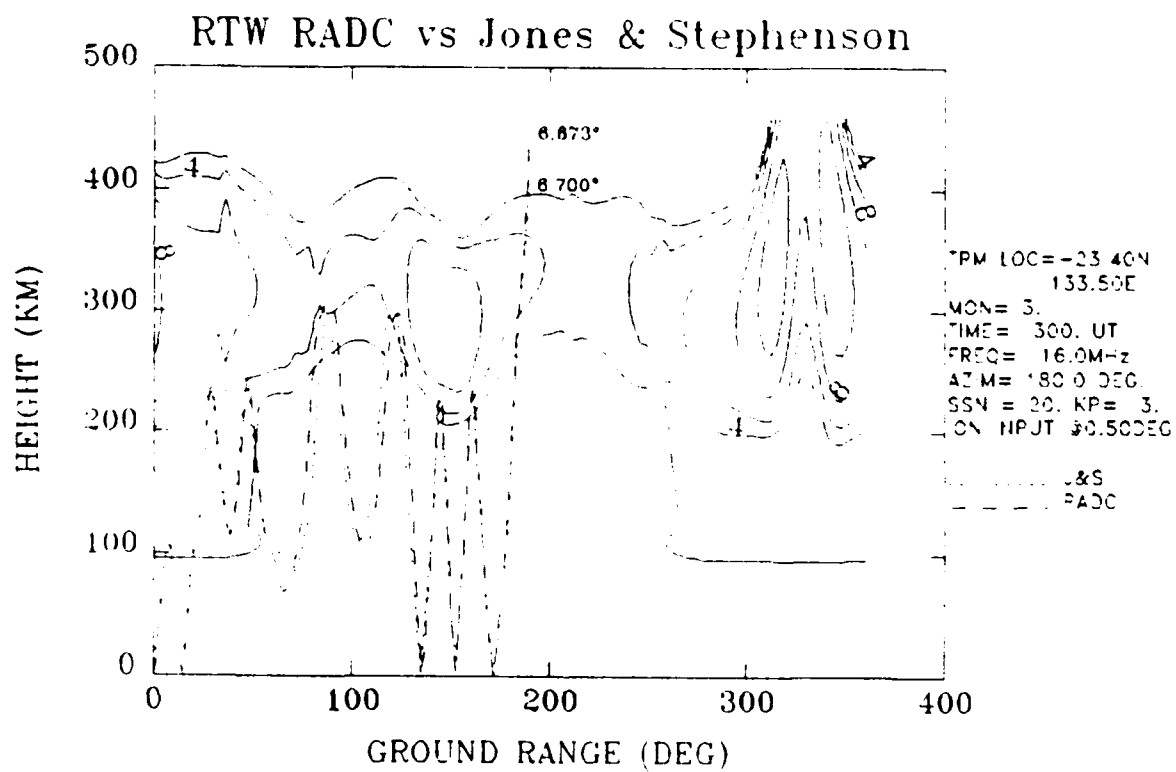


**Figure 8. Ray Traces Using Current Model vs Jones-Stephenson's<sup>1</sup> Program for Frequency = 16 MHz, Takeoff Angle = 6.7°.**

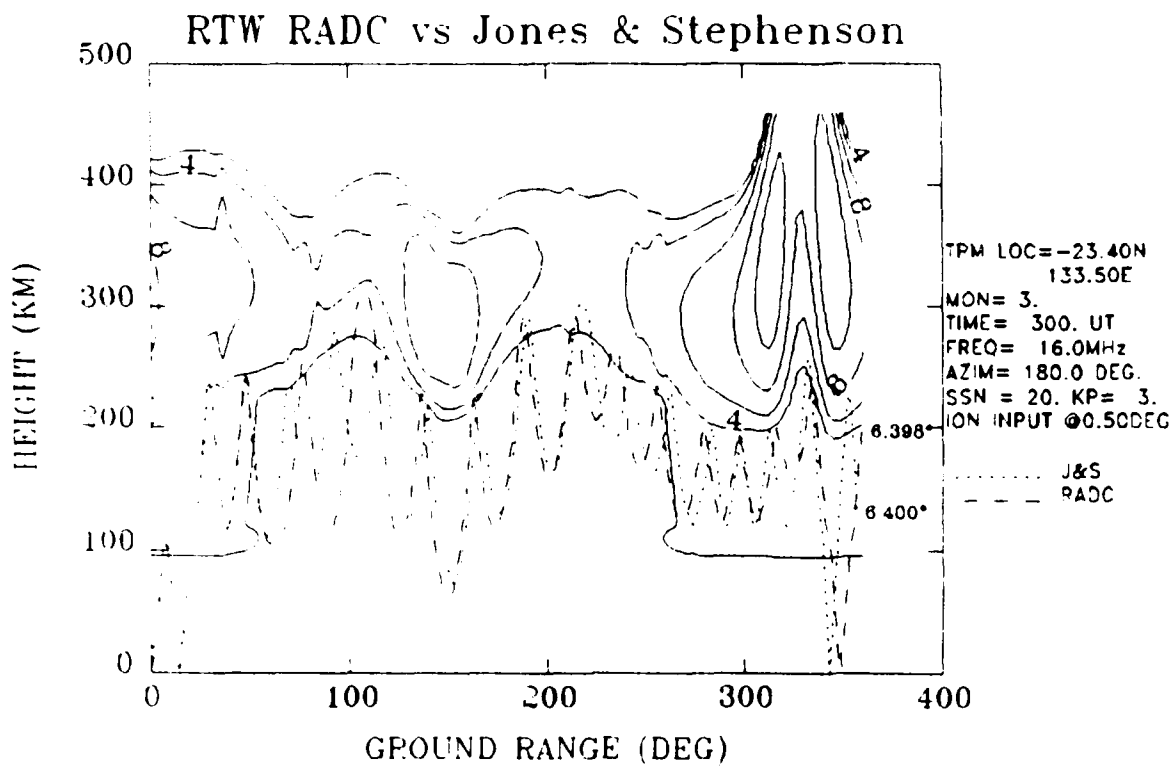


**Figure 9. Ray Traces Using Current Model vs Jones-Stephenson's<sup>1</sup> Program for Frequency = 16 MHz, Takeoff Angle = 6.4°.**

TRANSMITTER - ALICE SPRINGS, AUSTRALIA

TIME - 0300 UT

SEASON - MARCH EQUINOX

DIRECTION - DUE NORTH

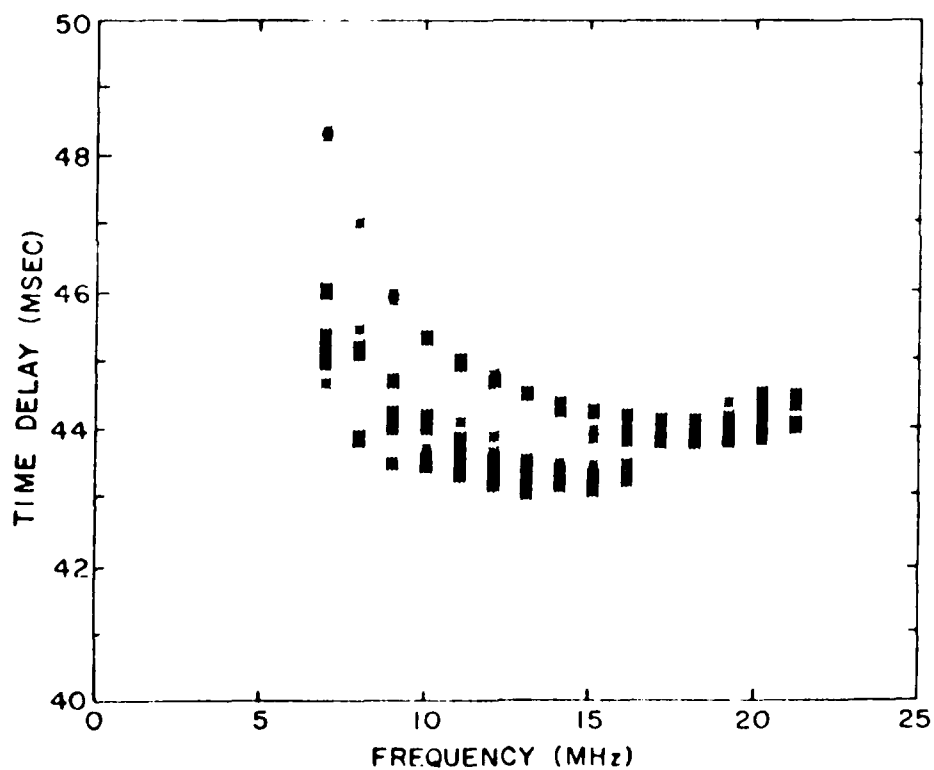


Figure 10. Ionogram Produced Using Current Ray Tracing Model with Transmitter Location and Time as Shown in Figure 7.

TRANSMITTER - ALICE SPRINGS, AUSTRALIA

TIME - 0300 UT

SEASON - MARCH EQUINOX

DIRECTION - DUE NORTH

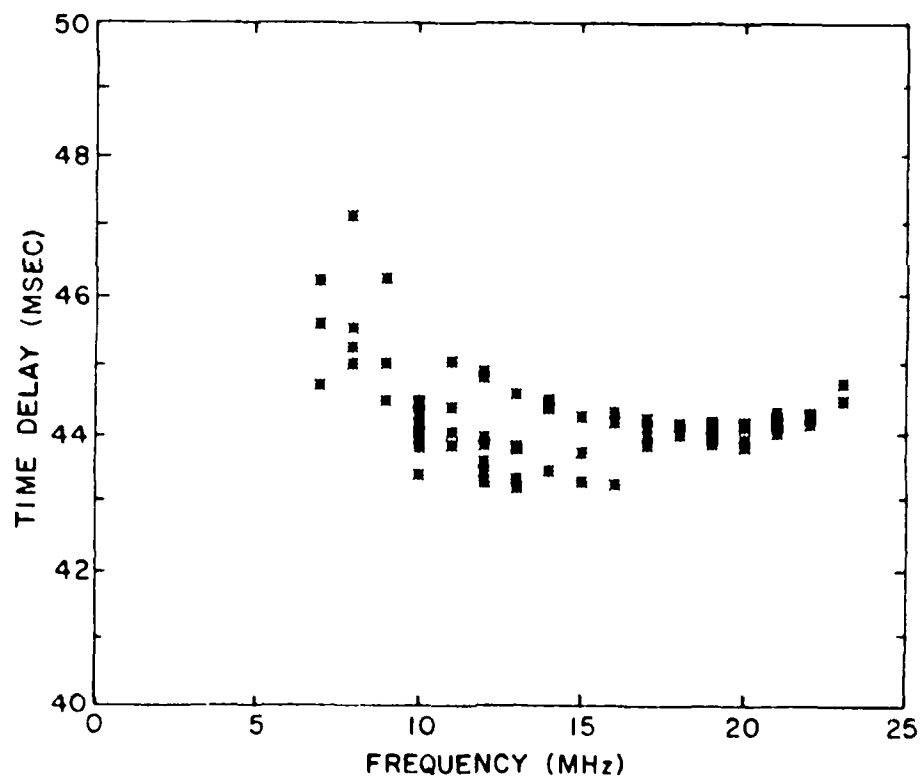


Figure 11. Ionogram Produced Using Jones-Stephenson<sup>1</sup> Program with Transmitter Location and Time as Shown in Figure 7.

## References

1. Jones, R.M., Stephenson, J.J. (1975) A Versatile Three-Dimensional Ray Tracing Computer Program for Radio Waves in the Ionosphere, *U.S. OT Report*, 75-76.
2. Ray, J.R. (1982) Exact Solutions to the Time-Dependent Schroedinger Equation, *Phys. Rev.*, **A26**:729/Hartley, J.G., Ray, J.R. (1981) Ermakov Systems and Quantum-Mechanical Superposition Laws, *Phys. Rev.*, **A24**:2873.
3. Lloyd, J.L., Haydon, G.W., Lucas, D.L., and Teters, L.R. (1984) Estimating the Performance of Telecommunications Systems Using the Ionospheric Transmission Channel, Vol. 1, *Techniques for Analyzing Ionospheric Effects Upon HF Systems*, NTIA/ITS.
4. Lewis, H.R., and Leach, P.G.L. (1982) Exact Invariants for Time-Dependent Nonlinear Hamiltonian Systems, *Nonlinear Problems: Present and Future*, Bishop, A.R., Campbell, D.K., and Nicolaenko, B. (eds) p. 133, North Holland.
5. Zheng, W.M. (1984) The Darboux Transformation and Solvable Double-Well Potential Models for Schroedinger Equations, *J. Math. Phys.*, **25**:88.
6. Nieto, M.M., Simmons, L.M. (1979) Coherent States for General Potentials III. Non-confining One-Dimensional Examples, *Phys. Rev. D*, **20**:1342.
7. Yukon, S.P. (1986) Calculation of Ray Paths in the Ionosphere Using an Analytic Ray Tracing Technique, RADC-TR-86-125, ADA178888.
8. Dhara, A.K., and Lawande, S.V. (1984) Feynman Propagators for Time Dependent Lagrangians Possessing an Invariant Quadratic in Momentum, *J. Phys. A*, **17**:2423.
9. Marcuse, D. (1974) Theory of Dielectric Optical Waveguides, *Academic Press*, New York.
10. Morse, P.M. (1929) Diatomic Molecules According to the Wave Mechanics II. Vibrational Levels, *Phys. Rev.*, **34**:57.
11. Schrodinger, E. (1926) *Naturwissenschaften*, **14**:664, English translation in Schrodinger, E. (1928) *Collected Papers on Wave Mechanics*, p. 41, Blackie & Son, London.

12. Nieto, M.M., Simmons Jr., L.M. (1979) Coherent States for General Potentials, I. Formalism, *Phys. Rev.*, **D20**:1321.
13. Gerry, C.C. (1986) Coherent States and a Path Integral for the Morse Oscillator, *Phys. Rev.*, **A33**:2207.
14. Ewing, W.M., Worzel, J.L. (1948) Long Range Sound Transmission, *Geol. Soc. Am. Mem.*, **27**, Part III, 1.
15. Quäck, E. (1927) Propagation of Short Waves Around the Earth, *Proc. IRE*, **15**:341. Further references in Toman, K. (1979) High-Frequency Ionospheric Ducting - A Review, *Radio Science*, **14**:447.
16. Brekhouskikh, L. and Lyzanov, Yu (1982) *Fundamentals of Ocean Acoustics*, Springer-Verlag, Berlin, Heidelberg, New York, p. 118.
17. Yukon, S.P. and Bendow, B. (1980) Design of Waveguides with Prescribed Propagation Constants, *J. Opt. Soc. Am.*, **70**:172.
18. Barton, G. (1986) Quantum Mechanics of the Inverted Oscillator Potential, *Ann. of Phys.*, **166**:322.





# MISSION of *Rome Air Development Center*

*RADC plans and executes research, development, test and selected acquisition programs in support of Command, Control, Communications and Intelligence (C<sup>3</sup>I) activities. Technical and engineering support within areas of competence is provided to ESD Program Offices (POs) and other ESD elements to perform effective acquisition of C<sup>3</sup>I systems. The areas of technical competence include communications, command and control, battle management information processing, surveillance sensors, intelligence data collection and handling, solid state sciences, electromagnetics, and propagation, and electronic reliability/maintainability and compatibility.*